

# Probing for cosmological parameters with LAMOST measurement

Hong Li<sup>a,b,c</sup>, Jun-Qing Xia<sup>a,d</sup>, Zuhui Fan<sup>c</sup>, and Xinmin Zhang<sup>a,b</sup>

<sup>a</sup>*Institute of High Energy Physics, Chinese Academy of Science, P.O. Box 918-4, Beijing 100049, P. R. China*

<sup>b</sup>*Theoretical Physics Center for Science Facilities (TPCSF), Chinese Academy of Science, P.R.China*

<sup>c</sup>*Department of Astronomy, School of Physics, Peking University, Beijing, 100871, P. R. China and*

<sup>d</sup>*Scuola Internazionale Superiore di Studi Avanzati, Via Beirut 2-4, I-34014 Trieste, Italy*

In this paper we study the sensitivity of the Large Sky Area Multi-Object Fiber Spectroscopic Telescope (LAMOST) project to the determination of cosmological parameters, employing the Monte Carlo Markov Chains (MCMC) method. For comparison, we first analyze the constraints on cosmological parameters from current observational data, including WMAP, SDSS and SN Ia. We then simulate the 3D matter power spectrum data expected from LAMOST, together with the simulated CMB data for PLANCK and the SN Ia from 5-year Supernovae Legacy Survey (SNLS). With the simulated data, we investigate the future improvement on cosmological parameter constraints, emphasizing the role of LAMOST. Our results show the potential of LAMOST in probing for the cosmological parameters, especially in constraining the equation-of-state (EoS) of the dark energy and the neutrino mass.

## INTRODUCTION

The measurement of the large scale galaxy clustering has been an important probe in constraining the cosmological models. The large scale structure (LSS) measurements have made remarkable progresses by the observational efforts such as 2dFGRS and Sloan Digital Sky Survey (SDSS), which have provided an accurate measurement of the galaxy power spectrum and given a robust constraint on cosmological parameters [1, 2].

The LAMOST [3] project is a 4m quasi-meridian reflecting Schmidt telescope laid down on the ground. It has a 5 degree field of view, and may accommodate as many as 4000 optical fibers and the light from 4000 celestial objects will be led into a number of spectrographs simultaneously. Thus the telescope will be the one that possesses the highest spectrum acquiring rate in the world. The spectroscopic survey which contains the information about the radial positions of galaxies, can probe the 3D distribution of galaxies effectively. In this paper, we study the sensitivity of LAMOST to the determination of cosmological parameters with the simulated galaxy power spectrum. In our analysis, we also consider the simulated observations for the future CMB and SN Ia measurements from PLANCK and the 5-year SNLS, which are presumably conducted during the same time period as LAMOST survey. Our results indicate that the LAMOST has the promising potential in probing for the cosmological parameters, especially in constraining on the EoS of the dark energy and the neutrino mass.

The paper is organized as follows: In Section II we describe the method of fitting and the simulation technique. In section III, we present the results and discussions. The last section contains a summary.

## METHODOLOGY

In this section, we introduce the method and the fitting procedure. For the dynamical dark energy model, we choose the parametrization given by [4]:

$$w(a) = w_0 + w_a(1 - a) , \quad (1)$$

where  $a = 1/(1+z)$  is the scale factor and  $w_a = -dw/da$  characterizes the “running” of the EoS (Run w henceforth). For the  $\Lambda$ CDM model,  $w_0 = -1$  and  $w_a = 0$ .

When using the MCMC global fitting strategy to constrain cosmological parameters, dark energy perturbations should be taken into account properly, especially for models with time evolving EoS of dark energy. This issue has been realized by many researchers including the WMAP group [5, 6, 7, 8]. However, when the parameterized EoS crosses  $-1$ , one cannot handle the dark energy perturbations based on quintessence, phantom, k-essence and other non-crossing models. By virtue of quintom [9], the perturbations at the crossing points are continuous. Thus we have proposed a technique to treat dark energy perturbations in the whole parameter space.

In this study, we have modified the publicly available Markov Chain Monte Carlo package CosmoMC[10] to include the dark energy perturbations. For handling the parametrization of the EOS getting across  $-1$ , firstly we introduce a small positive constant  $\epsilon$  to divide the full range of the allowed value of the EOS  $w$  into three parts: 1)  $w > -1 + \epsilon$ ;

2)  $-1 + \epsilon \geq w \geq -1 - \epsilon$ ; and 3)  $w < -1 - \epsilon$ . Working in the conformal Newtonian gauge, the perturbations of DE can be described by

$$\dot{\delta} = -(1+w)(\theta - 3\dot{\Phi}) - 3\mathcal{H}(c_s^2 - w)\delta \quad , \quad (2)$$

$$\dot{\theta} = -\mathcal{H}(1-3w)\theta - \frac{\dot{w}}{1+w}\theta + k^2\left(\frac{c_s^2\delta}{1+w} + \Psi\right) \quad . \quad (3)$$

Neglecting the entropy perturbation, for the regions 1) and 3), the EOS does not cross  $-1$  and the perturbation is well defined by solving Eqs.(2,3). For the case 2), the perturbation of energy density  $\delta$  and divergence of velocity,  $\theta$ , and the derivatives of  $\delta$  and  $\theta$  are finite and continuous for the realistic quintom DE models. However for the perturbations of the parameterizations, there is clearly a divergence. In our study for such a regime, we match the perturbations in region 2) to the regions 1) and 3) at the boundary and set

$$\dot{\delta} = 0 \quad , \quad \dot{\theta} = 0. \quad (4)$$

In our numerical calculations we limit the range to be  $|\Delta w = \epsilon| < 10^{-5}$  and find our method to be a very good approximation to the multi-field quintom. More detailed treatments can be found in Ref.[5, 6].

Furthermore, we assume purely adiabatic initial conditions and a flat universe. The parameter space we begin with for the numerical calculation is:

$$\mathbf{P} \equiv (\omega_b, \omega_c, \Theta_s, \tau, w_0, w_a, n_s, \ln(10^{10}A_s)) \quad , \quad (5)$$

where  $\omega_b \equiv \Omega_b h^2$  and  $\omega_c \equiv \Omega_c h^2$  with  $\Omega_b$  and  $\Omega_c$  being the baryon and cold dark matter densities relative to the critical density, respectively,  $\Theta_s$  is the ratio (multiplied by 100) of the sound horizon at decoupling to the angular diameter distance to the last scattering surface, and  $\tau$  is the optical depth. In Eq.(5),  $A_s$  and  $n_s$  characterize the power spectrum of primordial scalar perturbations. For the pivot scale of the primordial spectrum we set  $k_* = 0.05 \text{Mpc}^{-1}$ .

In our calculations, we take the total likelihood to be the products of the separate likelihoods ( $\mathcal{L}_i$ ) of CMB, LSS and SNIa. Defining  $\chi_{L,i}^2 \equiv -2 \log \mathcal{L}_i$ , we then have

$$\chi_{L,total}^2 = \chi_{L,CMB}^2 + \chi_{L,LSS}^2 + \chi_{L,SNIa}^2 \quad . \quad (6)$$

If the likelihood function is Gaussian,  $\chi_L^2$  coincides with the usual definition of  $\chi^2$  up to an additive constant corresponding to the logarithm of the normalization factor of  $\mathcal{L}$ .

The data used for current constraints include the three-year WMAP (WMAP3)<sup>1</sup> Temperature-Temperature (TT) and Temperature-Polarization (TE) power spectrum [13, 14, 15, 16] as well as the smaller scale experiments, including Boomerang-2K2 [17], CBI [18], VSA [19] and ACBAR [20], the SDSS luminous red galaxy (LRG) sample [1] and 2dFGRS [2], and recently released ESSENCE (192 sample) data [22, 23]. For the LSS power spectrum, we only use the data in the linear regime up to  $k \sim 0.1 h \text{Mpc}^{-1}$ . In the calculation of the likelihood from SNIa we have marginalized over the nuisance parameter [21]. Furthermore, we make use of the Hubble Space Telescope (HST) measurement of the Hubble parameter  $H_0 \equiv 100 h \text{ km s}^{-1} \text{ Mpc}^{-1}$  [24] by multiplying the likelihood by a Gaussian likelihood function centered around  $h = 0.72$  and with a standard deviation  $\sigma = 0.08$ . We also impose a weak Gaussian prior on the baryon density  $\Omega_b h^2 = 0.022 \pm 0.002$  ( $1 \sigma$ ) from the Big Bang Nucleosynthesis [25], and a cosmic age tophat prior as  $10 \text{ Gyr} < t_0 < 20 \text{ Gyr}$ .

For the future data, we consider the measurements of LSS from LAMOST, the CMB from PLANCK [26] and the SN Ia from 5-year SNLS[27].

For the simulation of LAMOST, we mainly simulate the galaxy power spectrum. We consider two sources of statical errors on the power spectrum measurements: the sample variance and the shot noises which due to the limited number of independent wavenumber sampled from a finite survey volume and the imperfect sampling of fluctuations by the finite number of the galaxies respectively,[28]

$$\left(\frac{\sigma_P}{P}\right)^2 = 2 \times \frac{(2\pi)^3}{V} \times \frac{1}{4\pi k^2 \Delta k} \times \left(1 + \frac{1}{\bar{n}P}\right)^2 \quad , \quad (7)$$

where  $V$  is the survey volume and  $\bar{n}$  is the mean galaxy density. From the more conservative estimation, we know that the redshift distribution of main sample of LAMOST is between 0 and 0.6 and the mean redshift is around 0.2.

---

<sup>1</sup> With the newly released 5-year WMAP data[11, 12], we have checked that the new data will not significantly change the results.

TABLE I. Constraints on cosmological parameters from the current observations and the future simulations. For the current constraints we have shown the mean values  $1\sigma$  (Mean) and the best fit results together. For the future mocked data we list the standard deviation (SD) of these parameters with fiducial model I (FMI) and fiducial model II (FMII). In order to highlight the contribution from LAMOST, we compare the results with/without LAMOST.

	Current for $\Lambda$ CDM		Future (SD with FMI)		Current for Run w		Future (SD with FMII)	
	Best Fit	Mean	PLANCK+ SNLS	PLANCK+ SNLS +LAMOST	Best Fit	Mean	PLANCK+SNLS	PLANCK+ SNLS +LAMOST
$w_0$	-1	-1	0.118	0.100	-1.16	$-1.03^{+0.15}_{-0.15}$	0.0899	0.0598
$w_a$	0	0	0.522	0.417	0.968	$0.405^{+0.562}_{-0.587}$	0.332	0.162
$\Omega_\Lambda$	0.760	$0.762^{+0.015}_{-0.015}$	0.0115	0.00547	0.756	$0.760^{+0.017}_{-0.018}$	0.0125	0.00460
$H_0$	73.1	$73.3^{+1.6}_{-1.7}$	1.594	0.828	70.3	$71.2^{+2.3}_{-2.3}$	1.840	0.673
$\sigma_8$	0.769	$0.755 \pm 0.031$	0.0223	0.0174	0.634	$0.675 \pm 0.068$	0.0299	0.0220

So for simplicity, in our study, we simulate the power spectrum of the galaxies at  $z = 0.2$  that can be got from these galaxies. The survey area is  $15000 \text{ deg}^2$  and the total number of galaxies within the survey volume is  $10^7$ [3]. We only consider the linear regime, namely the maximum  $k$  we consider is  $k \sim 0.1 \text{ h Mpc}^{-1}$ . As we know that, the galaxy power spectrum  $P(k)$  in EQ. (7) is

$$P(k) = b^2 p_m(k), \quad (8)$$

where  $p_m(k)$  is the linear matter power spectrum, and here we take  $b$  as a constant  $b = 1$  when simulating the data and when using the galaxy power spectrum to constrain cosmological parameters, we take  $b$  as a free parameter and marginalize over it.

For the simulation with PLANCK, we follow the method given in our previous paper [29]. We mock the CMB TT, EE and TE power spectrum by assuming the certain fiducial cosmological model. For the detailed techniques, please see our previous companion paper [29]. We have also simulated 500 SN Ia according to the forecast distribution of the SNLS [30]. For the error, we follow the Ref.[31] which takes the magnitude dispersion 0.15 and the systematic error  $\sigma_{sys} = 0.02 \times z/1.7$ . The whole error for each data is given by:

$$\sigma_{maga}(z_i) = \sqrt{\sigma_{sys}^2(z_i) + \frac{0.15^2}{n_i}}, \quad (9)$$

where  $n_i$  is the number of supernova of the  $i$ 'th redshift bin.

As pointed out in our previous works [32, 33, 34], the cosmological parameters are highly affected by the dark energy models due to the degeneracies among the EoS of DE and other parameters. Therefore, in our study of this paper, we choose two fiducial models with different dark energy properties:  $\Lambda$ CDM model (fiducial model I henceforth) and dynamical dark energy (fiducial model II henceforth) with time evolving EoS. The parameters of the two sets of fiducial models are obtained from the current observational data.

## RESULTS AND DISCUSSIONS

In Table I, we present the numerical results of the constraints on the cosmological parameters from the current data and the error forecast from the simulated data. To show the importance of LAMOST, we compare the two sets of results, one from PLANCK + SNLS, the other from PLANCK + SNLS + LAMOST. As we know, the matter power spectrum is directly related to the horizon size at matter-radiation equality, in turn the matter power spectrum will make accurate measurement of  $\Omega_m h$ . On the other hand, there are degeneracies between  $\Omega_m h$  and the other cosmological parameters, *e.g.*  $\Omega_\Lambda$ ,  $H_0$ ,  $w_0$ ,  $w_a$  and so on, hence the tight constraint on  $\Omega_m h$  will be helpful for breaking these degeneracies and improve the constraints on these cosmological parameters. For example, in Table I, one can find the constraints on  $\Omega_\Lambda$  and  $H_0$  are tightened a lot by including LAMOST. Also from Figure 1, one can see the constraints on the age of universe is also shrank obviously, this is because the age is directly related to the hubble constant and  $\Omega_m$ .

In figure 1, we plot the 2-D cross correlation and 1-D probability distribution of some of the basic cosmological parameters in Eq.(5) and also some of the reduced parameters. The black solid lines are given by fitting with the simulated PLANCK and SNLS, and the red solid lines are provided by including the simulated LAMOST data. From

TABLE II. Constraints on neutrino mass from the current observations and the future simulations. We have shown the  $2\sigma$  upper limits. In order to highlight the contribution from LAMOST, we compare the results with/without LAMOST.

Current		Future		
			PLANCK+SNLS	PLANCK+SNLS+LAMOST
$\Lambda$ CDM	$<0.958eV$	FMI	$<0.957eV$	$<0.377eV$
Run w	$<1.59eV$	FMII	$<0.915eV$	$<0.346eV$

the comparison, we find that LAMOST have promising potentials in constraining cosmological parameters, such as, the EoS of dark energy, the dark energy density budget  $\Omega_\Lambda$ , the age of universe,  $\sigma_8$  and the Hubble constant.

In order to see explicitly the effect of LAMOST on dark energy constraints, in figure 2, we plot the  $2\sigma$  confidence level contours on  $w_0$  and  $w_a$ . The black solid line is given by the current constraints and the red solid line is given by fitting with the simulated data of PLANCK and SNLS 5 year data with fiducial model II, while the red dashed line is given by including the simulated LAMOST data. This comparison shows clearly LAMOST will contribute significantly in tightening the constraints on the EoS of dark energy. Numerically we find the best fit model with the current data is given by the dynamical quintom model with EoS across -1, however the cosmological constant is within  $1\sigma$  confidence level. The future PLANCK measurement and 5-year SNLS SN Ia will be able to distinguish the cosmological constant from the dynamical model at  $2\sigma$  confidence level, while LAMOST can improve this sensitivity significantly at  $3.3\sigma$ . The blue solid lines and blue dashed lines show the comparison between the results with and without LAMOST for fiducial model I.

On the other hand, for the parameter related to the inflation models, such as  $n_s$  and  $A_s$ , the constraints are mainly from PLANCK, as pointed out in our previous paper[29]. Adding in LAMOST can not further tighten the constraints. We have also done another analysis with the additional parameters  $\alpha_s$  and  $r$ , and obtained the similar conclusion, where  $\alpha_s$  characterizes the running of the primordial power spectrum index and  $r$  is the ratio of tensor to scalar perturbations.

Now we study the cosmological constraint on the neutrino mass by adding in a new parameter  $f_\nu$  in Eq.(5). The parameter  $f_\nu$  is the dark matter neutrino fraction at present, namely,

$$f_\nu \equiv \frac{\rho_\nu}{\rho_{DM}} = \frac{\Sigma m_\nu}{93.105 eV \Omega_c h^2}, \quad (10)$$

where  $\Sigma m_\nu$  is the sum of the neutrino masses. In this study, the mocked data we use are generated by assuming the massless neutrino *i.e.*  $f_\nu = 0$  in the fiducial models. Consequently the constraints on  $f_\nu$  should be regarded as the upper limits of the neutrino mass which the future observations will be sensitive to. It is well known that the massive neutrinos modify the shape and amplitude of the matter power spectrum, and also the epoch of matter-radiation equality, angular diameter distance to the last scattering surface. Thus they leave imprints on the observations of CMB and LSS. In Table II, we provide the constraints on neutrino mass from the current observations and the future simulated data. For the current data<sup>2</sup>, within the framework of the  $\Lambda$ CDM model, we get  $\Sigma m_\nu < 0.958 eV$  (95%) which is consistent with the result in Ref.[1]. For the time evolving EoS of dark energy model, this limit is relaxed to  $\Sigma m_\nu < 1.59 eV$  (95%), due to the degeneracy between the dark energy parameters and the neutrino mass[33, 36].

With the simulated data, in figure 3, we illustrate the one dimensional probability distribution of the total neutrino mass  $\Sigma m_\nu$ . The black solid line is given by the current constraints, the red solid line is given by fitting with the simulated PLANCK + SNLS with fiducial model II and the red dashed line is given by including the simulated LAMOST. The blue solid line and blue dashed line are the results obtained with the fiducial model I. Our results show that the LAMOST can provide a more stringent constraint on the neutrino mass. For example, the  $2\sigma$  neutrino mass limit is changed from  $0.957eV$  to  $0.377eV$  by including the simulated LAMOST data with the fiducial model I.

---

<sup>2</sup> Usually Lyman- $\alpha$  data will give stringent constraint on the neutrino mass, however, its systematics are quite unclear currently. In our global analysis to be conservative, we have not included it [12, 35].

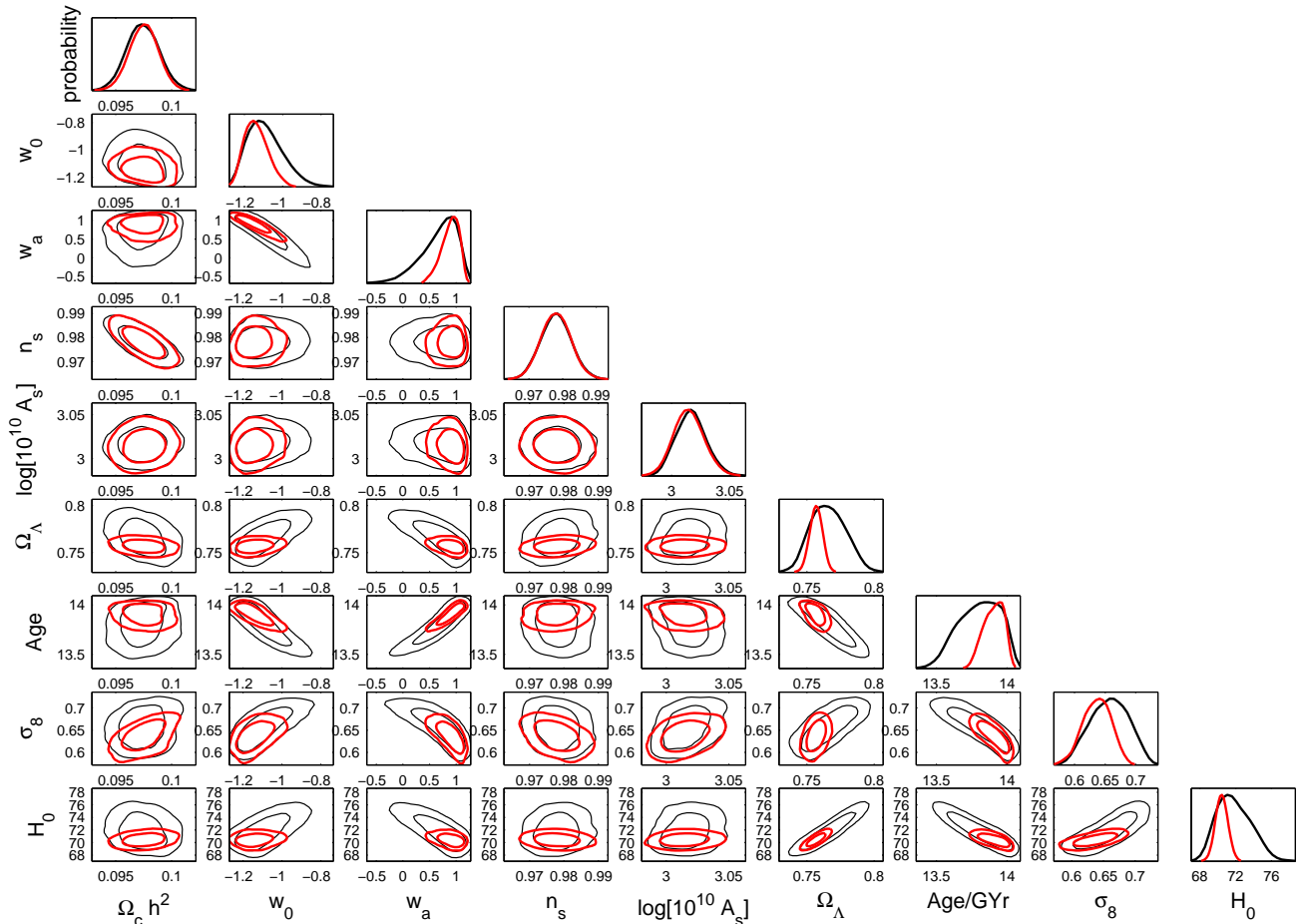


FIG. 1: one-dimensional distributions and two-dimensional 68% and 95% limits on the cosmological parameters. The black solid lines are obtained with the simulated PLANCK + SN Ia and the red solid lines are from PLANCK + SN Ia + LAMOST.

## SUMMARY

In this paper we have studied the sensitivity of LAMOST project to the determination of the cosmological parameters. With the simulated 3D matter power spectrum of LAMOST, in combination with the future PLANCK data and 5-year SNLS data, we have obtained the constraints on the various parameters by employing the MCMC method. Our results show the potential for LAMOST in constraining the cosmological parameters, especially on the EoS of dark energy and the neutrino mass.

We have performed our analysis in flat universe, however, if we take the curvature  $\Omega_k$  into consideration, namely if we free  $\Omega_k$  in the global analysis, the basic conclusion will not change. That is to say, we can also find the potential of the future LAMOST data in determining cosmological parameters, however, the specific contours of each cosmological parameters will be enlarged for the additional degree of freedom, and more relevant discussion can be seen in our previous paper[34], in which we have implemented the global fitting with the observational data for non-flat universe.

*Acknowledgement.* —

Our MCMC chains were finished in the Shuguang 4000A of the Shanghai Supercomputer Center (SSC). We thank Xuelei Chen, Bo Qin, Charling Tao, Lifan Wang, Pengjie Zhang, Yong-Heng Zhao, Zong-Hong Zhu, Tao-Tao Qiu and Lei Sun for discussions. This work is supported in part by China postdoctoral science foundation, National Science Foundation of China under Grant No. 10533010, and the 973 program No.2007CB815401, and by the Key Grant Project of Chinese Ministry of Education (No. 305001).

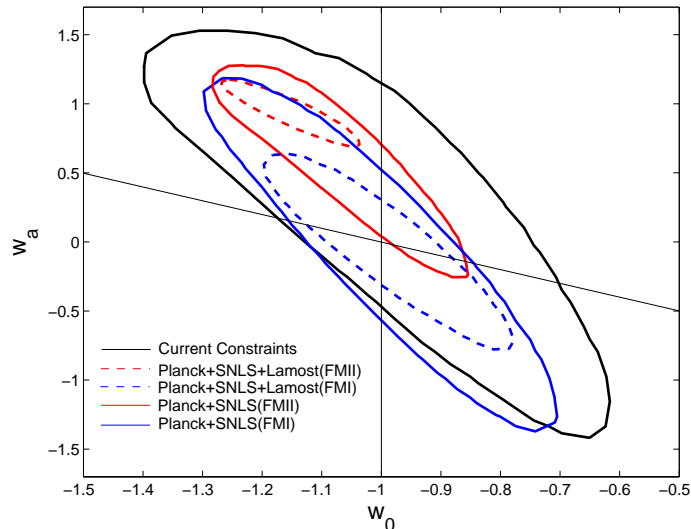


FIG. 2: 2-d joint 68% and 95% confidence regions of the parameters  $w_0$  and  $w_a$  for flat universe. The black solid line is given by the current constraints, the red solid line comes from the simulated data of PLANCK and 5year SNLS with fiducial model II, while the red dashed line is by combining the simulated LAMOST data. The blue solid line and blue dashed line are the results with the fiducial model I with/without LAMOST respectively.

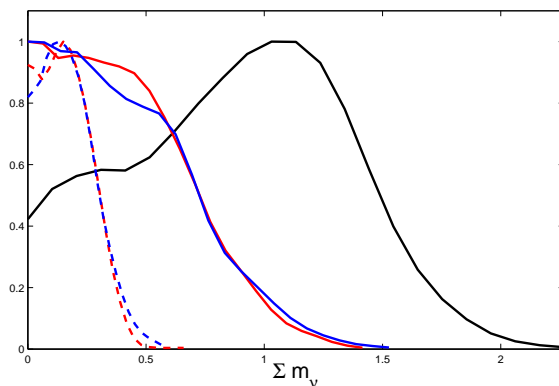


FIG. 3: one-dimensional constraints on the neutrino mass. The black solid line is given by the current data, the red solid line is given by fitting with the simulated PLANCK + SNLS with fiducial model II and the red dashed line is given by including the simulated LAMOST. The blue solid line and blue dashed line are the results obtained with the fiducial model I.

- 
- [1] M. Tegmark *et al.*, Phys. Rev. D **74**, 123507 (2006).  
[2] S. Cole *et al.*, Mon. Not. Roy. Astron. Soc. **362** (2005) 505.  
[3] <http://www.lamost.org/>  
[4] M. Chevallier and D. Polarski, Int. J. Mod. Phys. D **10**, 213 (2001); E. V. Linder, Phys. Rev. Lett. **90**, 091301 (2003).  
[5] G. B. Zhao, J. Q. Xia, M. Li, B. Feng and X. Zhang, Phys. Rev. D **72**, 123515 (2005).  
[6] J. Q. Xia, G. B. Zhao, B. Feng, H. Li and X. Zhang, Phys. Rev. D **73**, 063521 (2006).  
[7] D. N. Spergel *et al.*, Astrophys. J. Suppl. **170**, 377 (2007).  
[8] C. Yeche, A. Ealet, A. Refregier, C. Tao, A. Tilquin, J. M. Virey and D. Yvon, Astron. Astrophys. **448**, 831 (2006); J. Weller and A. Lewis, Mon. Not. Roy. Astron. Soc. **346**, 987 (2003).  
[9] B. Feng, X. L. Wang and X. M. Zhang, Phys. Lett. B **607**, 35 (2005).  
[10] A. Lewis and S. Bridle, Phys. Rev. D **66**, 103511 (2002); See also the CosmoMC website at: <http://cosmologist.info>.  
[11] G. Hinshaw *et al.*, arXiv: 0803.0732; M. R. Nolta *et al.*, arXiv: 0803.0593; J. Dunkley *et al.*, arXiv:0803.0586.  
[12] E. Komatsu, *et al.*, arXiv:0803.0547.  
[13] D. N. Spergel *et al.*, Astrophys. J. Suppl. **170**, 377 (2007).

- [14] L. Page *et al.*, *Astrophys. J. Suppl.* **170**, 335 (2007).
- [15] G. Hinshaw *et al.*, *Astrophys. J. Suppl.* **170**, 288 (2007).
- [16] N. Jarosik *et al.*, *Astrophys. J. Suppl.* **170**, 263 (2007).
- [17] C. J. MacTavish *et al.*, *Astrophys. J.* **647**, 799 (2006).
- [18] A. C. S. Readhead *et al.*, *Astrophys. J.* **609**, 498 (2004).
- [19] C. Dickinson *et al.*, *Mon. Not. Roy. Astron. Soc.* **353**, 732 (2004).
- [20] C. I. Kuo *et al.*, *Astrophys. J.* **600**, 32 (2004).
- [21] E. Di Pietro and J. F. Claeskens, *Mon. Not. Roy. Astron. Soc.* **341**, 1299 (2003).
- [22] G. Miknaitis *et al.*, arXiv:astro-ph/0701043.
- [23] T. M. Davis *et al.*, arXiv:astro-ph/0701510.
- [24] W. L. Freedman *et al.*, *Astrophys. J.* **553**, 47 (2001).
- [25] S. Burles, K. M. Nollett and M. S. Turner, *Astrophys. J.* **552**, L1 (2001).
- [26] Planck Collaboration, arXiv:astro-ph/0604069.
- [27] The SNLS Collaboration, *Astron. Astrophys.* **447**, 31(2006).
- [28] H.A. Feldman, N. Kaiser and J. A. Peacock, *APJ***426**, 23(1994).
- [29] J.-Q. Xia, H. Li, G.-B. Zhao and Xinmin Zhang, e-Print: arXiv:0708.1111
- [30] Ch. Yeche, et al., *Astron. Astrophys.* **448**, 831.
- [31] A. G. Kim, E. V. Linder, R. Miquel and N. Mostek, *Mon. Not. Roy. Astron. Soc.* **347**, 909 (2004).
- [32] J. Q. Xia, G. B. Zhao, B. Feng and X. Zhang, *JCAP* **0609**, 015 (2006).
- [33] J. Q. Xia, G. B. Zhao and X. Zhang, *Phys. Rev. D* **75**, 103505 (2007).
- [34] G. B. Zhao, J. Q. Xia, H. Li, C. Tao, J. M. Virey, Z. H. Zhu and X. Zhang, *Phys. Lett. B* **648**, 8 (2007).
- [35] G.L. Fogli, et al., arXiv:0805.2517.
- [36] S. Hannestad, *Phys. Rev. Lett.* **95**, 221301 (2005).